Food Chemistry: X 23 (2024) 101645

Contents lists available at ScienceDirect

Food Chemistry: X

journal homepage: www.sciencedirect.com/journal/food-chemistry-x

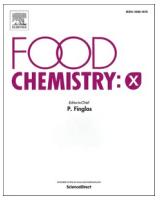

Regulated anthocyanin release through novel pH-responsive peptide hydrogels in simulated digestive environment

Wenjun Li [a,b,c], Qianqian Bie [a,b], Kaihui Zhang [a,b], Fangzhou Linli [a,b], Wenyu Yang [a,b,*], Xianggui Chen [a,b], Pengfei Chen [a,b], Qi Qi [a,b]

[a] School of Food and Bioengineering, Food Microbiology Key Laboratory of Sichuan Province, Xihua University, Chengdu, 611130, China
[b] Chongqing Key Laboratory of Speciality Food Co-built by Sichuan and Chongqing, Chengdu, 611130, China
[c] Frontiers Medical Center, Tianfu Jincheng Laboratory, Chengdu, 610212, China

ARTICLE INFO

Keywords:
Food nutrition delivery
Responsive hydrogel
Cyanidin
Controlled release

ABSTRACT

The instability of anthocyanins significantly reduces their bioavailability as food nutrients. This proof-of-concept study aimed to develop efficient carriers for anthocyanins to overcome this challenge. Characterization of the hydrogels via SEM (scanning electron microscope) and rheological analysis revealed the formation of typical gel structures. MTT (methyl thiazolyl tetrazolium) and hemolysis assays confirmed that their high biocompatibility. Encapsulation efficiency analysis and fluorescence microscopy images demonstrated successful and efficient encapsulation of anthocyanins by pH-responsive hydrogels. Stability studies further validated the effect of peptide hydrogels in helping anthocyanin molecules withstand factors such as gastric acid, high temperatures, and heavy metals. Subsequently, responsive studies in simulated gastric (intestinal) fluid demonstrated that the pH-responsive peptide hydrogels could protect anthocyanin molecules from gastric acid while achieving rapid and complete release in intestinal fluid environments. These results indicate that these peptide hydrogels could stabilize anthocyanins and facilitate their controlled release, potentially leading to personalized delivery systems.

1. Introduction

Anthocyanins (ANS), the naturally occurring antioxidants, hold immense potential in the food industry (Lang et al., 2021). However, their effectiveness is often compromised by environmental stressors, leading to their degradation and inactivation (Cai et al., 2022). This significantly reduces their nutritional benefits and bioavailability in food products. It is crucial to note that while anthocyanins are primarily absorbed in the human intestinal tract (in a pH range of 6.0–7.5), most of them become biologically inactive due to the acidic conditions of the gastric environment, with a pH of 0.9–1.5 (Wang, Dong, et al., 2023; Wang, Li, et al., 2023). This results in minimal absorption and utilization by the body, as Gui et al. (2023) highlighted. Therefore, this study focuses on how to use appropriate biomaterials to protect anthocyanins from gastric acidity and ensure their effective release in the small intestine.

Two critical factors must be considered in the design of delivery materials to achieve targeted anthocyanin release in the intestinal fluid. First, the delivery agent needs to possess excellent stability to protect anthocyanins against environmental hazards, such as gastric acids and metal ions (Zhao et al., 2020). Second, the material must adapt or respond within the small intestine to facilitate the release and absorption of anthocyanins into the body. Recent advancements have highlighted hydrogels as a promising solution, an efficient and gentle biomaterial for transporting bioactive compounds, including anthocyanins (Jin et al., 2020). Hydrogels can protect bioactive molecules in acidic conditions through their distinct three-dimensional networks. Moreover, hydrogels can demonstrate physical changes in different pH environments (Hu & Ying, 2023). For instance, they can exhibit alterations in swelling behavior and structural porosity in alkaline conditions. This unique property of hydrogels enables their controlled release of compounds like anthocyanins, making them a promising solution for targeted delivery. For example, Liu et al. (2022) successfully encapsulated anthocyanins in a gelatin/gellan gum-based hydrogel to shield them from gastric acidity. The structure of the designed hydrogel becomes less stable in the intestinal environment, thus promoting the release of anthocyanins where they can be absorbed. Similarly, Ozel et al. (2020) utilized the distinct swelling properties of peptide-enriched

* Corresponding author at: School of Food and Bioengineering, Food Microbiology Key Laboratory of Sichuan Province, Xihua University, Chengdu 611130, China
E-mail address: yangwenyu@mail.xhu.edu.cn (W. Yang).

https://doi.org/10.1016/j.fochx.2024.101645
Received 27 May 2024; Received in revised form 4 July 2024; Accepted 9 July 2024
Available online 14 July 2024

whey protein isolate (WPI) across acidic and alkaline conditions to develop a novel hydrogel carrier. This carrier provides stable encapsulation and ensures the controlled release of anthocyanin-rich black carrot concentrate in the intestinal tract.

These findings emphasize that the responsiveness of hydrogel materials to gastric and intestinal fluids is a critical factor in the controlled release efficiency of ANS (Yang et al., 2023). Maximizing the stability of the ANS-hydrogel complex in gastric fluids while minimizing its residual structure in intestinal fluids is essential for the controlled release of ANS within the hydrogel materials, thereby enhancing its bioavailability. Importantly, given the stringent biocompatibility standards in food and biology, only biocompatible materials that meet these criteria can be developed as functional carriers for the controlled release of anthocyanins.

As endogenous biological molecules, peptides exhibit high biocompatibility without producing any harmful metabolic byproducts. Research on peptide-based hydrogel materials has shown promising results in stabilizing bioactive molecules like anthocyanins (Li et al., 2023). Although no current reports exist on the controlled release of anthocyanins using peptide materials, peptides have been validated as safe and effective carriers for bioactive compounds such as hesperidin (Tai et al., 2023), curcumin (Altunbas et al., 2011), and resveratrol (Kim et al., 2020). Therefore, the objective of this study is to develop novel responsive polypeptide hydrogel materials that can effectively encapsulate and stabilize natural anthocyanin molecules, improve their stability in acidic gastric environments, and ensure their full release in intestinal fluids.

Specifically, in this study, we leveraged the adaptive charge properties of the acidic amino acids Asp (D) and Glu (E), which are uncharged in acidic environments but carry a negative charge in neutral or slightly alkaline conditions. Based on that, we designed two novel pH-responsive peptide hydrogel carriers: Fmoc-FDFD (F-FDFD) and Fmoc-FEFE (F-FEFE), and proposed the following hypothesis: in gastric fluids (acidic environment), the D and E remain uncharged, rendering the peptide carrier electrically neutral. This neutrality promotes the parallel alignment of peptide molecules, forming a gel structure that effectively encapsulates anthocyanins within its three-dimensional matrix, shielding them from environmental stressors such as stomach acid and metal ions. On the contrary, in the intestinal fluids (slightly alkaline environment), the carboxyl groups of D and E acquire a negative charge, resulting in heightened electrostatic repulsion between peptide molecules. This repulsive force effectively destroys the alignment of the peptide, resulting in the gel's disintegration and the encapsulated compounds' complete release. (Fig. 1).

Thus, we first synthesized pH-responsive peptide hydrogels with sensitive pH-responsive properties to validate our hypothesis. Then, we comprehensively characterized the hydrogels' gelation properties using Scanning Electron Microscopy and rheological analysis. We also performed rigorous biocompatibility tests through MTT and hemolysis toxicity analysis. Furthermore, we employed fluorescence microscopy and Fourier-transform infrared Spectroscopy (FT-IR) to assess their encapsulation efficiency for anthocyanins and quantified the encapsulation rate using a pH differential method. Additionally, we explored their protective role against environmental stresses such as high temperatures and metal ions. Finally, the pH-responsive release characteristics of anthocyanins were assessed in simulated gastric and intestinal fluids.

Our findings validate our hypothesis and hold significant implications for practical applications. The novelty of our research can be summarized as follows: firstly, the use of peptide hydrogel materials to stabilize and responsively release anthocyanins in gastrointestinal environments can significantly enhance the bioavailability of anthocyanins, offering a solution for delivering food nutrition molecules like anthocyanins. Secondly, the design of peptide hydrogels based on the pH responsiveness of electronegative amino acids D and E allows for rapid and effective responses in different pH environments and simulated gastrointestinal conditions. This design ensures the complete release of anthocyanins in intestinal fluids, avoiding any residuals within the gel material. Additionally, the pH-responsive peptide hydrogels designed in this study exhibit different pH responses and physicochemical properties based on the type of amino acid used. Considering the variability in gastrointestinal pH among different populations, the potential for personalized and efficient anthocyanin delivery through engineered peptide hydrogel carriers with varying pH responsiveness is fascinating,

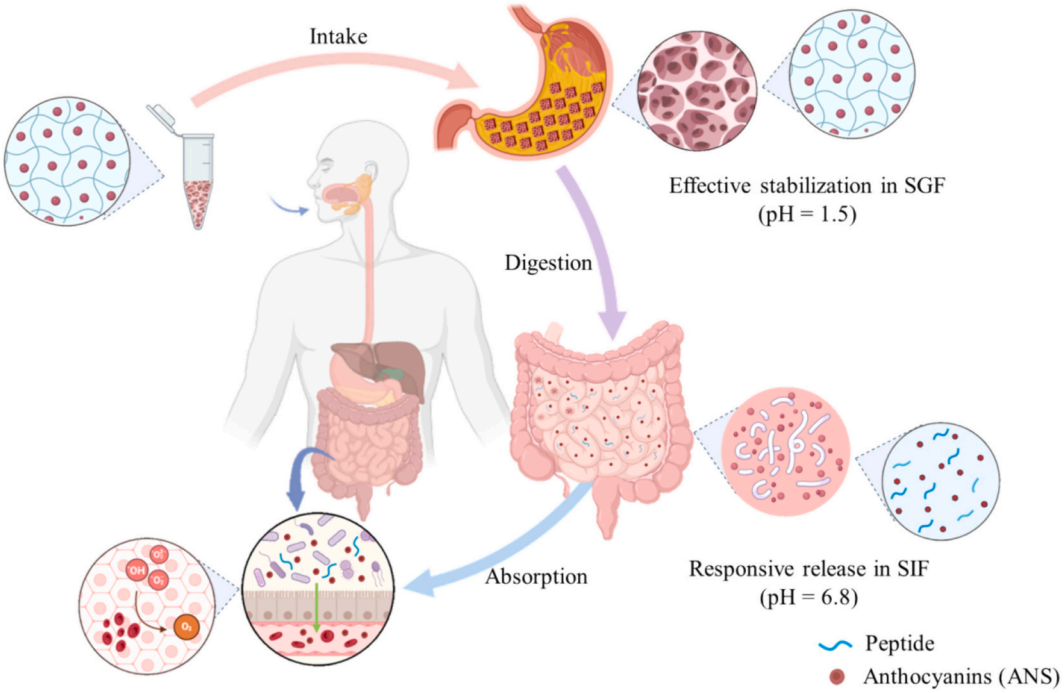

Fig. 1. Schematic presentation of this study that demonstrates the successful stability and controlled release of anthocyanins using pH-responsive peptide hydrogels in a simulated digestive environment (SGF: simulated gastric fluid; SIF: simulated intestinal fluid).

which could be achieved by further exploring a range of peptide gel carrier systems.

2. Materials and methods

2.1. Materials

The primary reagents used in this study and their suppliers were as follows: Morphine, triisopropylsilane (TIS), trifluoroacetic acid (TFA), dimethyl sulfoxide (DMSO), phosphate-buffered saline (PBS), glucono delta-lactone (GDL), and N,N-diisopropylethylamine were purchased from Energy Chemical Co., Ltd.(Chengdu China); methanol, chlorine dioxide, *N*,*N*-dimethylformamide, ether, hydrochloric acid, potassium chloride, sodium dihydrogen phosphate, citric acid, and sodium carbonate were purchased from Chengdu Kelong Chemical Co., Ltd. (Chengdu, China); MBHA resin (loading capacity of 0.674 mmol/g) and fmoc-protected amino acids were purchased from Nanjing Peptide Biotechnology Co., Ltd.(Nanjing, China); anthocyanin (mulberry source, purity 25%) was purchased from Xi'an Shengqing Biotechnology Co., Ltd.(Xi'an, China); Artificial gastric fluid (pH 1.5) and artificial intestinal fluid (pH 6.8) were purchased from Shanghai Yuanye Biotechnology Co., Ltd. (Shanghai China). CCK8 assay kit was purchased from Biosharp (company), DMEM medium, fetal bovine serum, penicillin, streptomycin, and cell culture dishes were purchased from Thermo Fisher Scientific company (Massachusetts, USA). HeLa cells were obtained from ATCC and cultured in DMEM medium supplemented with 10% (*v*/v) fetal bovine serum, 100 μg/mL penicillin, and 100 μg/mL streptavidin. Cells were grown at 37 °C, 5% CO2, in cell culture dishes.

The main instruments and equipment used in this study were: HPLC (LC-20, Shimadzu), LCMS (Agilent LCMS 1260–6120, Agilent), Laser granmeter (Zetasizer Nano ZS, Malvern), Scanning electron microscopy (Apreo2C, Thermo Scientific, America), Rheology analysis(MCR 302, Anton Paar, China), Fluorescence microscopy image (Ti—S, Nikon, Japan), Fourier-transform infrared spectroscopy (PerkinElmer Life and Analytical Sciences, Boston, MA, USA), Microplate reader (Feyond-A400,China).

2.2. Peptide synthesis

The peptides Fmoc-FEFE (F-FEFE) and Fmoc-FDFD (F-FDFD) were synthesized using the standard Fmoc solid-phase peptide synthesis (SPPS) method. Trifluoroacetic acid (TFA), ultrapure (Up) water, and trifluoroacetic acid (TIS) were mixed in a 95: 2.5: 2.5 ratio and stirred for two hours to get the peptides out of the resin. Subsequently, the resin was filtered, and the cleavage solution was dried using N_2 gas. The resulting peptides underwent drying and HPLC purification after ice ether precipitation. LC-MS was employed for peptide identification. Finally, the purified peptides were freeze-dried and stored at −20 °C.

2.3. Preparation of pH-responsive peptide hydrogels

Fmoc-FDFD (F-FDFD): A solution of Fmoc-FDFD peptide (5 mg) in ultrapure water (200 μl) was sonicated for 5 min to dissolve. Then, 10 mg of glucono-β-lactone (GDL) was added. The mixture was stirred and left to sit until a pH-responsive peptide hydrogel formed.

Fmoc-FEFE (F-FEFE): peptide (5 mg) was dissolved in ultrapure water (200 μl) with sodium carbonate (10 μl) as a solubilizer. The solution was sonicated for 5 min, and then GDL (10 mg) was added. The mixture was vortexed and left to stand to obtain a pH-responsive peptide hydrogel.

Using pH-responsive peptide hydrogels to encapsulate anthocyanin: GDL (10 mg) and anthocyanin (1 mg) were dissolved in the appropriate solvents, and then they were mixed with the peptide solutions in the same way as above.

2.4. Characterization of pH-responsive peptide hydrogels

2.4.1. Zeta potential analysis of peptide molecules

Two peptide solutions and a control solution were prepared to evaluate their zeta potentials. The F-FDFD peptide solution included 5 mg of peptide powder, 10 μL of 4 mol/L sodium carbonate, and 875 μL of ultrapure water. The F-FEFE peptide solution was made with the same components in identical proportions. The control solution comprised 10 μL of 4 mol/L sodium carbonate and 990 μL of ultrapure water. These solutions were then measured at room temperature using a Zetasizer Nano ZS (Malvern) to determine the zeta potential of the peptides in an alkaline medium.

2.4.2. Scanning electron microscopy (SEM)

According to the method outlined in Section 2.3, 5 mg each of F-FDFD and F-FEFE peptides were combined with ultrapure water at room temperature to form gels. These gels were frozen at −80 °C and dried to produce peptide gel powders. Then, 1 mg of the dried peptide gel was mounted using a conductive adhesive coated with gold nanoparticles. The microstructure of the hydrogels was then examined with a scanning electron microscope (SEM) (Apreo2C, Thermo Scientific).

2.4.3. Rheology analysis

The strength and stability of the pH-responsive peptide hydrogels were assessed by measuring their rheological properties using a rheometer (MCR 302, Anton Paar, China) with a 25-mm probe. For this analysis, 220 mg of F-FDFD and F-FEFE peptide hydrogels were placed on the rheometer base. Oscillatory amplitude sweeps were performed on both hydrogel samples, with strain ranging from 0.01% to 100% at a constant frequency of 1 Hz. This exploration allowed us to determine the different peptide hydrogels' storage modulus (G'), loss modulus (G"), and phase angle values. The mechanical stability of the pH-responsive peptide gels was measured by tracking changes in G' and G" values under 0.1% strain and an angular frequency range of 0.1 to 100 rad/s.

2.5. Biocompatibility evaluation of pH-responsive peptide hydrogels

2.5.1. Cell cytotoxic evaluation

The cell viability of pH-responsive peptide hydrogels was measured by the CCK8 assay, following the previously reported method (Li et al., 2018). HeLa cells (1×10^4 cells) with good viability were cultured overnight in a CO_2 incubator after seeding into a 96-well plate. The hydrogels were then immersed in PBS (1 mL) at 37 °C for 4 h to produce hydrogel leachates. These leachates were transferred to the wells with the cultured HeLa cells and incubated for 24 h. The negative control was the DMEM medium without hydrogel leachates. The medium was removed from all wells and replaced with fresh medium (100 μl) containing CCK8 solution. The solution was incubated at 37 °C for 3 h, and its optical absorbance was recorded at 450 nm using a microplate reader (SpectraMax 13×, Molecular Devices, USA). The impact of the hydrogel on the growth viability of HeLa cells was then evaluated with the following formula:

$$\text{Cellular vitality} = \frac{A_{sample}}{A_{negative\ cotrol}} \times 100\%$$

2.5.2. Hemolysis toxicity evaluation

The hemolytic toxicity of peptide hydrogels was measured using fresh mouse blood cells, following the method of (Li et al., 2018). The pH-responsive peptide hydrogels were incubated with PBS (1 mL, pH 7.4) at 37 °C for 4 h, and the hydrogel permeates were collected. The permeates were neutralized with sodium carbonate and filtered through a 0.22 μm membrane. The hydrogel permeate (500 μl) was incubated with fresh blood cells (5×10^7 cells/mL) at 37 °C for 1.5 h. The negative control was PBS solution, and the positive control was 0.1% SDS. The mixture was centrifuged at 1000 rpm for 10 min, and the supernatant

was collected. The absorbance of the supernatant at 540 nm was recorded using a microplate reader (SpectraMax 13×, Molecular Devices, USA), and the hemolytic toxicity of the pH-responsive peptide hydrogels was computed using the following formula:

$$\text{Hemolytic ratio}(\%) = \frac{A_{sample} - A_{negative}}{A_{positive} - A_{negative}} \times 100$$

where A_{sample} represents the absorbance of peptide hydrogel, A_{negative} represents the absorbance of negative control (PBS), and A_{positive} represents the absorbance of positive control (0.1% SDS).

2.6. Investigation of the encapsulation effect of pH-responsive peptide hydrogels

2.6.1. Determination of anthocyanins content

The pH differential method (He et al., 2017) was used to determine the anthocyanin content. The anthocyanin solution was diluted with buffer solutions of potassium chloride (0.025 M, pH = 1.0) and sodium acetate (0.4 M, pH = 4.5). In a microplate, 180 μL of each buffer solution and 20 μL of the centrifuged sample were added. The absorbance of the solutions was measured at 520 nm and 700 nm using a microplate reader. The formula below was used to calculate the anthocyanin content, which consists of the following variables: MW (molecular weight of anthocyanin - 449.2 g/mol), DF (dilution multiple), V (volume of liquid to be measured), ε (extinction coefficient - 26,900 mol/l × cm), and L (light range - 1 cm).

$$\text{C}(\text{mg/L}) = \frac{[(A_{520} - A_{700})]\text{pH}_{1.0} - (A_{520} - A_{700})\text{pH}_{4.5} \times \text{M}_\text{W} \times \text{DF} \times 1000 \times \text{V}}{\varepsilon \times \text{L}}$$

2.6.2. Measurement of encapsulation efficiency

The encapsulation efficiency of the peptide-anthocyanin hydrogel was assessed by the method reported by Jeong and Na (2012), with a little modification. The hydrogel was made with 1 mg of anthocyanins derived from mulberry, and 1 mL of ultrapure water was added to the gel (refer to Section 2.3). The mixture was stirred and shaken thoroughly, and the supernatant was obtained by a 0.45 μm filter membrane. The anthocyanin content in the supernatant was quantified as per Section 2.6.1. The encapsulation efficiency of the peptide hydrogel for anthocyanins was computed with the following formula:

$$\text{Encapsulation Efficiency}(\%) = \frac{\text{Total anthocyanins} - \text{Surface anthocyanins}}{\text{Total anthocyanins}} \times 100$$

2.6.3. Fluorescence microscopy image

As described in Section 2.3, the peptide hydrogel was prepared and infused with mulberry anthocyanins. This peptide-anthocyanin hydrogel was then frozen at −80 °C and freeze-dried. The lyophilized powder was placed on a slide and exposed to green laser light. An inverted fluorescent microscope (Ti—S, Nikon, Japan) was used to observe the microstructural morphology of the hydrogel and any changes induced by the anthocyanin loading. The encapsulation efficiency of the anthocyanins within the peptide hydrogel was also assessed.

2.6.4. Fourier-transform infrared spectroscopy (FT-IR) analysis

The peptide hydrogel loaded with anthocyanins was freeze-dried at −80 °C. The dried powder was mixed with anhydrous KBr powder in a 1:100 ratio and pressed into pellets for analysis. Following this, an infrared spectrometer (PerkinElmer Life and Analytical Sciences, Boston, MA, USA) was employed for analysis. Infrared absorption spectra were obtained by scanning 32 times across the spectral range of 4000–400 cm^{-1}.

2.7. Evaluation of anthocyanin stability enhancement by pH-responsive peptide hydrogels

2.7.1. Thermal stability

Following the methods described in previous research (Cui et al., 2024), the free anthocyanin solution was used as a control while the peptide-anthocyanin hydrogel was heated to 80 °C in a water bath for 5 h. The samples were then allowed to cool to room temperature. Next, 1 mL of ultrapure water was added to the prepared hydrogel, mixed thoroughly, and centrifuged. The supernatant was collected, and its anthocyanin content was quantified as described in Section 2.6.1. Moreover, the stability of anthocyanins in the peptide hydrogel was calculated using the following formula:

$$\text{Retention rate}(\%) = \frac{M_{Final\ anthocyanins}}{M_{initial\ anthocyanins}} \times 100$$

2.7.2. Cu^{2+} stability

Drawing upon previously published literature for analytical evaluation methods (Yao et al., 2021), peptide-anthocyanin hydrogels were subjected to a 3-h incubation in a $CuCl_2$ (10 mM and 50 mM) solution, with a free anthocyanin solution serving as the control. Subsequently, the residual anthocyanin content was determined according to the procedure outlined in Section 2.6.1. The anthocyanin retention (%) was calculated using the formula provided in Section 2.7.1, aiming to analyze and assess the effect of the peptide hydrogel samples on enhancing the stability of anthocyanins in the presence of metal ions.

2.7.3. Na^+ and K^+ stability

Peptide anthocyanin hydrogels were separately incubated in 1 M NaCl and KCl solutions for 2 h, followed by centrifugation for 5 min (1000 rpm) to collect the supernatant. Subsequently, the released anthocyanin content was determined according to the method outlined in Section 2.6.1. The release rate of anthocyanins was calculated using the following formula to assess the stability of peptide hydrogel carriers in high ionic strength environments.

$$\text{Release rate}(\%) = \frac{M_{released\ anthocyanins}}{M_{initial\ anthocyanins}} \times 100$$

2.7.4. Storage stability

According to the methods set up by Luo et al. (2019), the same amount of peptide-anthocyanin hydrogel and free anthocyanin solution were kept in separate containers at room temperature for 46 days with or without any light. After that, the method from Section 2.6.1 was used to find out how much anthocyanin was still in the peptide-anthocyanin hydrogel and the free anthocyanin solution. Then, the formula from Section 2.7.1 was used to figure out how much anthocyanin was retained. This was done to study and figure out how peptide hydrogels affected the stability of anthocyanins in storage.

2.7.5. Effects of peptide hydrogels on antioxidant activity of anthocyanin

The impact of peptide-anthocyanin hydrogels on the antioxidant activity of natural anthocyanins was investigated following the methodology outlined by Bobinaitė et al. (2012). Peptide-anthocyanin hydrogels were incubated at 50 °C for 72 h, with a free anthocyanin solution serving as the control. Subsequently, 100 μl of the supernatant from each sample was taken and added to 200 μl of ethanol solution containing DPPH (0.4 mM), followed by incubation at room temperature in the dark for 30 min. Absorbance at 517 nm was then measured, and the scavenging efficiency of each sample towards DPPH radicals was calculated using the formula below, aiming to analyze and evaluate the influence of peptide hydrogels on the antioxidant activity of anthocyanins:

$$\text{DPPH reduction}(\%) = \left(1 - \frac{A_1 - A_2}{A_0}\right) \times 100\%$$

where

A_0 is the absorbance at 517 nm of the blank (200 μl DPPH ethanol +100 μl ethanol).
A_1 is the absorbance at 517 nm of the sample (200 μl DPPH ethanol +100 μl anthocyanin).
A_2 is the absorbance at 517 nm of the sample without DPPH (200 μl + 100 μl anthocyanin).

2.8. Controlled anthocyanin release by pH-responsive peptide hydrogels in human gastric (intestinal) fluid environment

Adopting the experimental protocol outlined by Ahmad et al. (2018), simulated gastric fluid was prepared by dissolving 2.5 g of pepsin in 200 mL of ultrapure water, adjusting the pH to 2.0 with dilute hydrochloric acid, and then adjusting the volume to 250 mL with ultrapure water. Simulated intestinal fluid was prepared by dissolving 1.7 g of potassium dihydrogen phosphate in 100 mL of ultrapure water and 2.5 g of pancreatin in 100 mL of ultrapure water, combining the two solutions, adjusting the pH to 7.4 with sodium hydroxide solution, and then adjusting the volume to 250 mL with ultrapure water. Samples of 200 mg of peptide Fmoc-FDFD and Fmoc-FEFE anthocyanin hydrogels (containing 1 mg of anthocyanin) were individually immersed in 2 mL of simulated gastric fluid (pH = 1.5) or simulated intestinal fluid (pH = 7.4) environments. Subsequently, they were gently agitated at 37 °C (20 rpm/min) for thorough mixing. After incubation for different durations (30, 60, 90, and 120 min) in simulated gastric fluid, the supernatant was collected, and the residual anthocyanin content was determined using the methodology described in Section 2.6.1. Anthocyanin retention was then calculated following the procedures outlined in Section 2.7.1. This analysis aimed to assess the pH-responsive, controlled release of anthocyanin molecules by Fmoc-FDFD and Fmoc-FEFE peptide hydrogels. In simulated intestinal fluid, due to the rapid responsiveness of the peptide hydrogels, nearly 100% anthocyanin release efficiency could be measured after just 10 min of incubation using the abovementioned method.

2.9. Statistical analysis

All experiments were repeated three times, and the results are reported as the mean ± standard deviation (SD). Statistical analysis was conducted using one-way analysis of variance (ANOVA). Graphs were generated using Origin 2018 (OriginLab Co. Ltd., Northampton, USA). The statistical significance levels were indicated as follows: ns (not significant), $*p < 0.05$, $**p < 0.01$, $***p < 0.001$.

3. Results and discussion

In this proof-of-concept study, we have developed two innovative pH-responsive peptide hydrogels, namely F-FDFD (Fmoc-FDFD) and F-FEFE (Fmoc-FEFE), capitalizing on the pH-responsive nature of negatively charged amino acids D and E. The primary objective is to ensure the stability of anthocyanins in gastric acid and facilitate their complete release into the intestinal environment. To achieve this, we initiated the synthesis of two peptides through standard -Fmoc solid-phase peptide synthesis (SPSS) techniques. Subsequently, purification was carried out using reversed-phase high-performance liquid chromatography (HPLC), and the identity of the target peptides was confirmed via LC-MS analysis (refer to supporting information).

3.1. Exploration of pH-responsive behavior

We first investigated the formulated peptide hydrogels' gelation properties and pH-responsive behavior. Fig. 2 illustrates the spontaneous formation of uniform and stable hydrogels by F-FDFD and F-FEFE under acidic conditions, as indicated by the yellow color of the bromocresol green pH indicator. Conversely, under alkaline conditions, both peptides exist in peptide solutions, as is evident by the blue color of the pH indicator. Notably, both pH-responsive peptide hydrogels exhibit high sensitivity to pH changes, transitioning from gel to solution state within 1 min (A recorded video showcasing this phenomenon is available for readers in the supporting information). These observations underscore the significant responsiveness of the designed peptide hydrogels to acidic and alkaline environments. Furthermore, we measured the zeta potential of peptides in an alkaline environment to validate our hypothesis. As illustrated in **Fig. S1**, F-FDFD and F-FEFE exhibited significantly enhanced electronegativity compared to the control group, indicating that peptides carry negative charges in alkaline environments. The electrostatic repulsion between peptides carrying similar negative charges further disrupts the parallel arrangement of hydrophobic aromatic groups within the peptides (e.g., side-chain groups of F and Fmoc), ultimately dissolving peptide gel structures (Tena-Solsona et al., 2014).

Subsequently, employing a pH meter, we accurately determined the critical pH values for the gelation of the two pH-responsive peptide hydrogels. The critical pH for gelation was 5.64 for F-FDFD and 6.81 for F-FEFE. These findings suggest that both pH-responsive peptide hydrogels can remain stable in the human gastric fluid environment (pH = 0.9–1.5) while losing their gel state in the human intestinal fluid environment (approximately pH 7.6 in the small intestine and pH 8.3–8.4 in the large intestine). This rapid response mechanism could facilitate the swift and controllable release of food nutrients, such as anthocyanins.

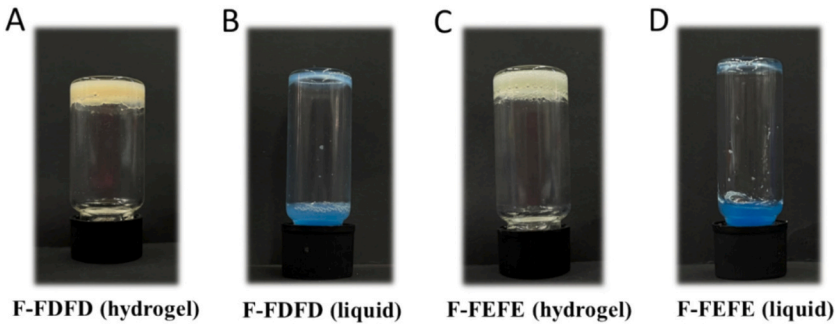

Fig. 2. The morphological images of pH-responsive peptide hydrogels under different pH conditions (bromocresol green pH indicator: yellow color signifies pH < 3.8, while blue color represents pH > 5.4). (A) Fmoc-FDFD in an acidic environment (hydrogel); (B) Fmoc-FDFD in an alkaline environment (solution); (C) Fmoc-FEFE in an acidic environment (hydrogel); (D) Fmoc-FEFE in an alkaline environment (solution). (For interpretation of the references to color in this figure legend, the reader is referred to the web version of this article.)

3.2. Microstructure characterization

Subsequently, we characterized the microstructures of the two pH-responsive peptide hydrogels using scanning electron microscopy (SEM). As demonstrated in Fig. 3, both F-FDFD and F-FEFE exhibit a typical three-dimensional porous hydrogel structure reminiscent of the microstructure reported by Wei et al. (2019). This three-dimensional porous gel structure is crucial for facilitating bioactive molecules' loading and delivery (Mandru et al., 2019). These findings further validate the gel structures formed by peptide molecules from a microscopic perspective, implying their potential applications in stabilizing and achieving controlled release of anthocyanins.

3.3. Rheological analysis

As potential carriers for anthocyanins, adequate mechanical properties are required to withstand various physical stressors during processing and intake. Therefore, we conducted a rheological analysis to investigate the mechanical properties of two novel pH-responsive peptide hydrogels. As shown in Fig. 4A-4B, the amplitude sweep results reveal that the storage modulus (G') significantly exceeds the loss modulus (G"), approximately tenfold higher than the loss modulus (G"). These results indicate the formation of stable, rigid hydrogel structures by both peptide molecules, demonstrating rheological characteristics typical of an elastic solid (Dong et al., 2022).

Furthermore, we conducted frequency sweep studies on the two peptide hydrogels. Within the linear viscoelastic region, with strain maintained at a constant 0.1%, we measured the storage modulus (G') and loss modulus (G″) as functions of angular frequency, allowing for the analysis of the hydrogel's viscoelasticity and network properties (Wang, Dong, et al., 2023; Wang, Li, et al., 2023). As depicted in Fig. 4C-4D, within the frequency range of 0.1 to 100 rad/s, hydrogels exhibited minimal fluctuations in storage modulus (G′) and loss modulus (G″) with frequency, indicating weak dependency. These findings suggest that both peptide molecules have formed stable gel structures with high storage modulus (G') and mechanical strength, which can aid in protecting food nutrients such as anthocyanins against various physical stressors.

3.4. Biocompatible evaluation

Biocompatibility is crucial in designing materials loaded with anthocyanins (Song et al., 2022). To verify the robust biocompatibility of our pH-responsive peptide gel material, we undertook additional investigations into its cellular-level biotoxicity using MTT assays and hemolysis tests. In the cell culture environment for 24 h, HeLa cells were exposed to the exudates of the two peptide hydrogels, as shown in Fig. 5A. The cells displayed a favorable growth status, with their cellular activity even slightly surpassing that of the control group (DMEM). These results collectively suggest the absence of significant cytotoxicity from the two peptide hydrogels.

The hemolysis assay effectively evaluates the blood cell compatibility of biomaterials by assessing red blood cell lysis and hemoglobin dissociation (Peng et al., 2011). As demonstrated in Fig. 5B and **Fig. S2**, after a 1.5-h co-incubation of fresh mouse blood cells with peptide hydrogels at 37 °C, no apparent damage to the blood cells was observed in the peptide group compared to the positive control (0.1% SDS). Notably, there was no significant increase in the absorbance of the supernatant at 540 nm. These findings suggest the absence of significant hemolytic toxicity associated with the two peptide hydrogels. In summary, cell toxicity and hemolysis assays confirm the high biocompatibility of the two pH-responsive peptide hydrogels, positioning them as promising novel materials for anthocyanin encapsulation.

3.5. Anthocyanins encapsulation

It is crucial to ensure sufficient loading onto peptide hydrogels to achieve controlled release and enhance the bioavailability of anthocyanin molecules. Therefore, we examined the capability of two designed peptide hydrogels to load anthocyanins and assessed their encapsulation efficiency. As shown in **Fig. 6C** and **E**, following the mixing of anthocyanins with peptide, the peptide hydrogels exhibited a distinct red coloration compared to their initial state, indicating the successful integration of anthocyanins into the peptide hydrogels. Subsequently, we employed the pH differential method to determine the encapsulation efficiency of the two hydrogels for anthocyanins. Encouragingly, the encapsulation efficiencies of anthocyanins by the two peptide hydrogels were impressively high, reaching 99.71 ± 0.09% and 98.27 ± 0.87%, respectively. Notably, in the supernatant post-loading onto the peptide hydrogels, there was hardly any observable red color indicative of anthocyanin molecules (Fig. 6C, E). These findings highlight the efficient loading capacity of the designed peptide hydrogels for anthocyanin molecules.

3.6. Anthocyanins distribution in peptide-anthocyanins hydrogels

Subsequently, we employed inverted fluorescence microscopy to investigate the distribution of anthocyanins within the two responsive peptide hydrogels. As depicted in Fig. 7, both F-FDFD and F-FEFE exhibited a shattered glass-like crystalline structure after freeze-drying, consistent with the microstructure previously reported for hydrogels (Jiang et al., 2023). Moreover, the anthocyanins displaying red fluorescence were evenly dispersed within the shattered glass crystalline structure of the peptide hydrogels, showing no significant aggregation, indicating efficient encapsulation of anthocyanins by the peptide hydrogels, which aligns with observations reported by (Zhang et al., 2017).

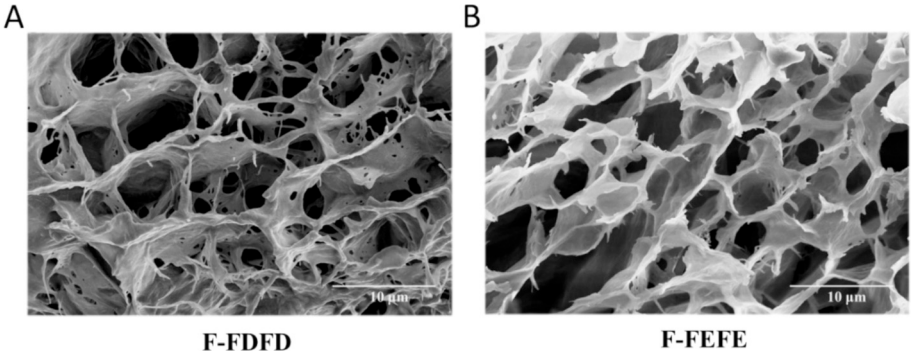

Fig. 3. Micromorphology characterization of two novel pH-responsive peptide hydrogels.

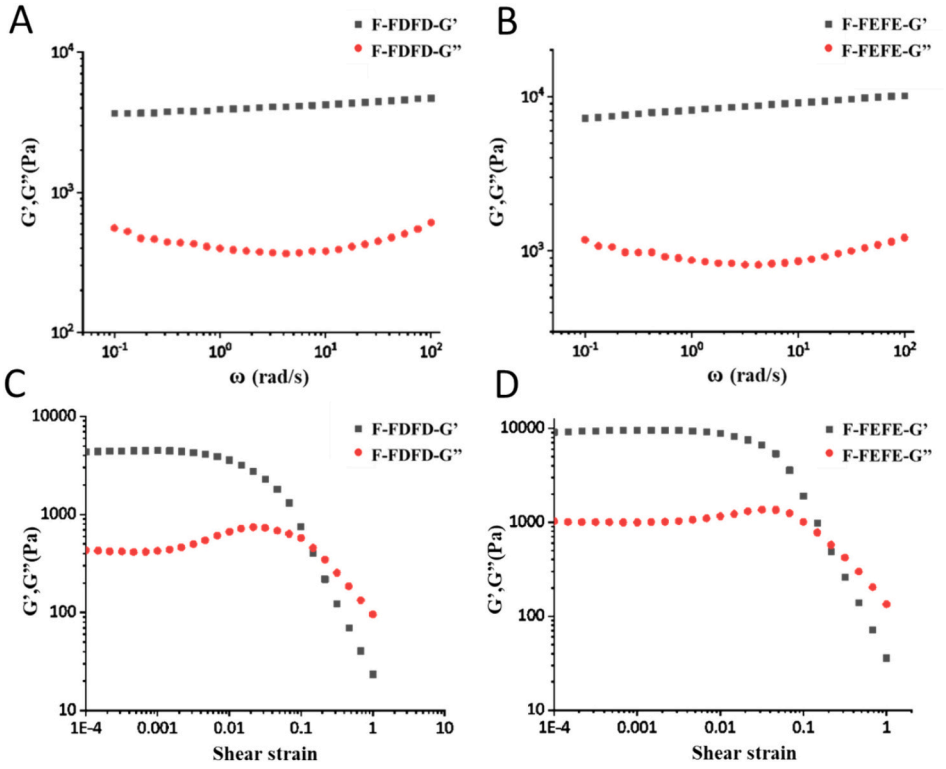

Fig. 4. Rheological analyses of pH-responsive peptide hydrogels. (A, B) Amplitude sweep analysis of peptide hydrogel F-FDFD and F-FEFE; (C, D) Frequency sweep analysis of peptide hydrogel F-FDFD and F-FEFE.

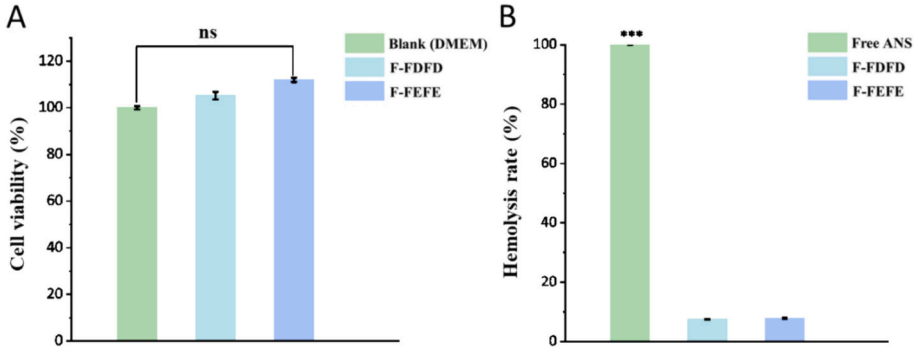

Fig. 5. Biocompatible evaluation of the novel pH-responsive peptide. (A) MTT analysis; (B) Hemolysis analysis. The results were analyzed by one-way analysis of variance (ANOVA), and the level of significance were indicated as: ns (no significance), and ***$p < 0.001$.

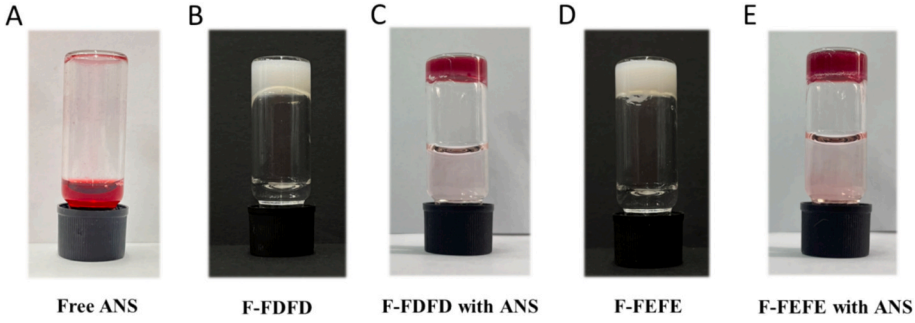

Fig. 6. Exploring pH-responsive peptide hydrogels as innovative encapsulation materials for anthocyanins.

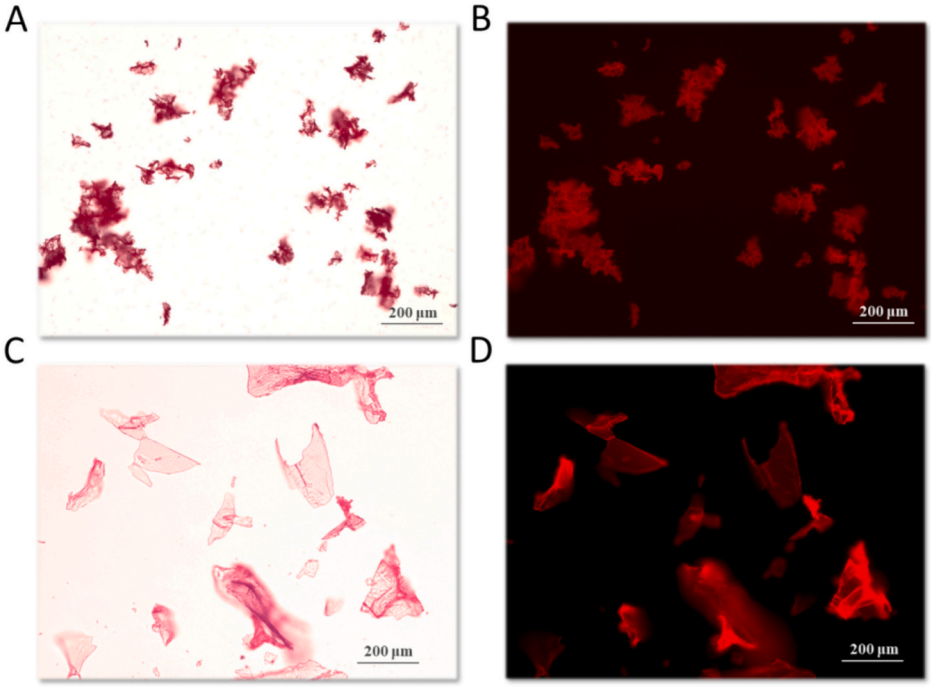

Fig. 7. Inverted fluorescent microscopic imaging of encapsulated anthocyanin in peptide hydrogels. (A, B) Fmoc-FDFD; (C, D) Fmoc-FEFE. Both exhibited a uniform and intense red fluorescence attributable to anthocyanin. (For interpretation of the references to color in this figure legend, the reader is referred to the web version of this article.)

3.7. Fourier transform infrared spectroscopy (FT-IR) analysis

Subsequently, we employed Fourier-transform infrared spectroscopy (FT-IR) to character the biophysical properties of the novel pH-responsive peptide hydrogels. As illustrated in **Fig. S3**, the infrared absorption spectrum of anthocyanins exhibited characteristic peaks: a band at 3390 cm^{-1} corresponding to the stretching vibration of O—H bonds, an absorption band at 1620 cm^{-1} originating from the stretching vibration of C—C bonds in the aromatic ring, a weak absorption peak at 1078 cm^{-1} arising from the stretching and bending vibrations of the C-O-C bonds in the aromatic ring, which are typical features of flavonoid compounds, and a strong absorption band at 1022 cm^{-1} attributed to the vibrational absorption of C—H bonds in the aromatic ring, consistent with the infrared spectral characteristics of anthocyanins observed by Zhao et al. (2021). In the infrared spectrum of the peptide hydrogels, the characteristic peak at 3292 cm^{-1} represents the stretching vibration of the peptide backbone N—H bonds and the presence of intermolecular hydrogen bonds between peptide backbone N—H groups. The absorption peaks at 1644 cm^{-1} and 1675 cm^{-1} correspond to the typical absorption of C═O double bonds in the peptide amide groups (Bardajee et al., 2020). In comparison to peptide hydrogels without loaded anthocyanins, hydrogels loaded with F-FDFD and F-FEFE anthocyanins exhibited a significant enhancement in the absorption peaks at 1037 cm^{-1}, indicating successful encapsulation of anthocyanin molecules by the peptides, consistent with our previous observations (Li et al., 2023).

3.8. Evaluation of anthocyanin stability improved by peptide hydrogels

Achieving controlled release of anthocyanins within the gastrointestinal tract requires protection against stressors such as gastric acid and metal ions (Zhang et al., 2023), ensuring safe transit to the intestinal environment for absorption (Victoria-Campos et al., 2022). Thus, we examined the capability of two pH-responsive peptide hydrogels to protect anthocyanins from such stressors. As depicted in **Fig. S4**, both peptide hydrogels exhibited significantly higher residual anthocyanin levels after a 5-h incubation at 80 °C compared to free anthocyanin aqueous solutions ($p < 0.001$). These results indicate the ability of both peptide hydrogels to improve anthocyanin stability under high-temperature conditions.

Additionally, heavy metal ions like Cu^{2+} in the environment often induce precipitation or discoloration reactions of anthocyanins, diminishing their bioavailability (Yao et al., 2021). Therefore, we further investigated the impact of peptide hydrogels on aiding anthocyanins in resisting Cu^{2+} metal ion stress. As depicted in Fig. 8A, under the stress of a 50 mM $CuCl_2$ solution, the free anthocyanin solution's residual rate was merely 29.4% ± 0.26%. In contrast, the retention rates of anthocyanins in the two pH-responsive peptide hydrogels exceeded 60%, specifically 79.5% ± 0.31% (F-FDFD) and 64.2% ± 2.46% (F-FEFE), respectively. These results indicate that these two novel peptide hydrogels can assist anthocyanin molecules in resisting the effects of heavy metal ion stress.

Moreover, the presence of prevalent metal ions such as K^+ and Na^+ may lead to the disruption and fragmentation of the gel structure at high concentrations. Consequently, this may result in the premature release of anthocyanin molecules stabilized within the three-dimensional network of the peptide hydrogel. Thus, we further investigate the stability of peptide hydrogels (loaded with ANS) in such environments with 1 M K^+ and Na^+ solutions. As depicted in **Fig. 8B**, F-FDFD, and F-FEFE maintained distinct gel morphologies even after incubation in K^+ and Na^+ environments for 2 h. Notably, minimal anthocyanin release was observed in the supernatant, with the anthocyanin release ratios being 5.14% ± 0.32% (F-FDFD in K^+ environment) and 5.78% ± 1.2% (F-FEFE in K^+ environment), 6.2% ± 0.29% (F-FDFD in Na^+ environment) and 5.35% ± 0.60% (F-FEFE in Na^+ environment). These results indicate that both novel peptide hydrogel carriers can maintain their gel structure in high ionic strength environments and protect the encapsulated anthocyanin molecules.

In addition, we investigated their long-term stabilizing effect on natural anthocyanins. As shown in Fig. 8C and **Fig. S5**, after 46 days of storage at room temperature, the anthocyanin retention encapsulated by peptide hydrogels was significantly higher than that of free anthocyanins. These results indicate that these novel peptide hydrogels can serve

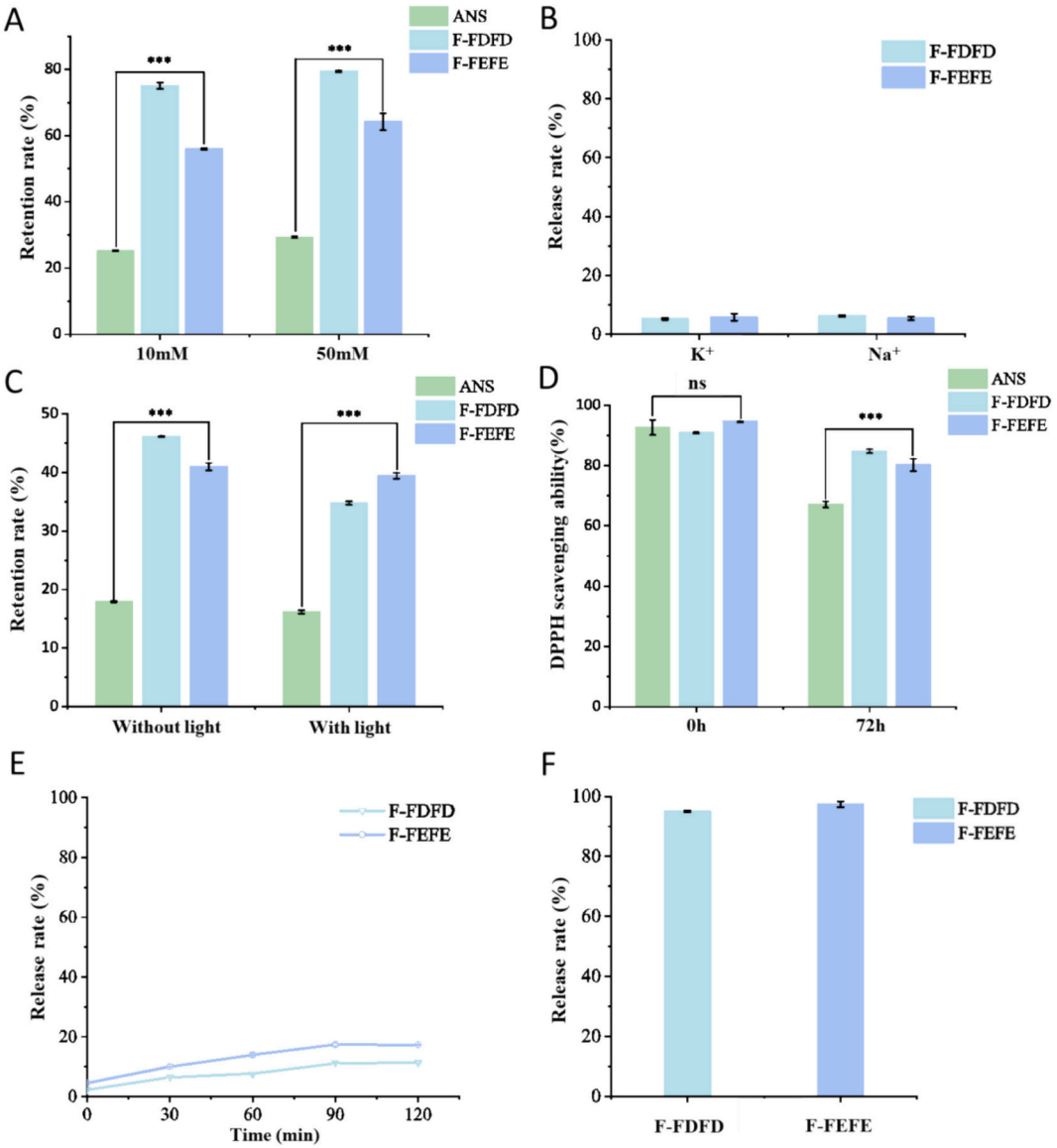

Fig. 8. Investigation of the stabilizing effect of pH-responsive peptide hydrogels on anthocyanins and their responsiveness in simulated gastrointestinal digestion. (A) Anthocyanin stabilization under Cu^{2+} metal stress (10 mM and 50 mM); (B) Hydrogel (loaded with ANS) stabilization under K^+ and Na^+ metal stress (1 M); (C) Long-term storage stability at room temperature (46 days); (D) Protective effect on anthocyanin antioxidant activity (DPPH) at 50 °C; (E) Effective stabilization of anthocyanin in stimulated gastric fluid (SGF) for 2 h; (F) Rapid and complete release of anthocyanin by pH-responsive peptide hydrogels in simulated intestinal fluid (SIF) in 10 min. The results were analyzed by one-way analysis of variance (ANOVA), and the level of significance were indicated as: ns (no significance), and ***$p < 0.001$.

as promising materials for extended anthocyanin storage.

Antioxidant activity represents one of anthocyanins' most critical biological functions as essential nutritional molecules in food. Therefore, we further examined the effectiveness of peptide hydrogels in protecting the antioxidant activity of anthocyanins under temperature stress. As shown in Fig. 8D, the free anthocyanin samples lost a lot of their ability to remove DPPH after being incubated at 50 °C for 72 h. However, the anthocyanins that F-FDFD and F-FEFE protected kept their ability to remove DPPH much higher ($p < 0.001$). The findings show that both pH-responsive peptide hydrogels could effectively preserve the antioxidant activity of anthocyanins.

3.9. Responsive release in gastrointestinal fluid environment

As an essential nutritional molecule, anthocyanins cannot be absorbed in the stomach and are rendered biologically inert by the acidic gastric environment, significantly diminishing their bioavailability (Gui et al., 2023). The central issue in the design of anthocyanin carriers lies in assisting anthocyanins in resisting the adverse effects of the gastric environment and achieving their complete release in the intestinal environment. Thus, we investigated the responsiveness of two anthocyanin-loaded pH-responsive peptide hydrogels in simulated gastric and intestinal fluids. As shown in Fig. 8E and **Fig. S5**, both F-FDFD and F-FEFE peptide hydrogels kept their gel shapes after incubating at 37 °C for 2 h in simulated gastric fluid (SGF). There was a clear boundary between the gastric fluid and the peptide gel. The clear supernatant demonstrated that anthocyanin release from the gel structure was minimal. The pH differential method showed that the anthocyanin content was 11.4 ± 0.25% (F-FDFD) and 17.3 ± 0.12% (F-FEFE), respectively. This phenomenon indicated that the anthocyanin stayed stable in the gel structure in the simulated gastric fluid. However, only after 10 min of incubation in simulated intestinal fluid (SIF), the gel structures of both peptide hydrogels completely disappeared, resulting in a homogeneous red solution (**Fig. S6**). The pH differential analysis

revealed a significant difference ($p < 0.001$) in release rates, with 95.04 ± 0.24% (F-FDFD) and 97.36 ± 0.98% (F-FEFE), respectively (Fig. 8F). These results demonstrated the effective release of natural anthocyanin from the peptide gel structure in the intestinal fluid environment.

Therefore, our research on pH-responsive peptide hydrogels as carriers for anthocyanins is significant. These hydrogels protect anthocyanins from environmental stressors like metal ions and gastric acid, facilitating their rapid and effective release in the intestinal fluid environment. This enhanced bioavailability of anthocyanin could potentially revolutionize their absorption by the human body, thereby optimizing their nutritional benefits in food applications.

4. Conclusions

In summary, we hypothesize that the pH sensitivity of amino acids D and E can induce the pH responsiveness of peptide hydrogels, thereby enabling the controlled release of natural anthocyanin molecules in simulated gastrointestinal fluids. Our experiments demonstrate that in the acidic environment of gastric fluid, both F-FDFD and F-FEFE hydrogels could maintain their structural integrity and effectively stabilize anthocyanin molecules. Conversely, in the alkaline environment of intestinal fluid, the pH responsiveness of D or E molecules causes the hydrogel structure to degrade, leading to the complete release of the encapsulated anthocyanin molecules. These findings validate our initial hypothesis. It is worth noting that although both novel pH-responsive peptide hydrogel carriers exhibit similar and commendable gel properties and anthocyanin delivery efficiency in simulated intestinal fluid environments ex vivo, considering the gradient pH distribution in the gastrointestinal tract in vivo, we anticipate that peptide hydrogel carriers with different pH responsiveness would result in distinct anthocyanin loading and delivery efficiencies. For example, the pH-responsive slightly acidic peptide hydrogel F-FDFD (pH 5.64) might achieve earlier ANS release during the initial stages of digestion compared to the pH-responsive slightly alkaline peptide hydrogel F-FEFE (pH 6.81), thereby yielding diverse ANS delivery efficiencies. Furthermore, given the variability in pH environments across different populations' digestive tracts, the potential for personalized, efficient ANS delivery needs by engineering ANS peptide hydrogel carriers with varying pH responsiveness in the future is a fascinating prospect. Thus, we anticipate and aspire to establish a range of peptide gel carrier systems with varying pH-responsive activities in the future, leveraging the modifiability of peptide molecules. Such systems would facilitate the effective delivery of diverse nutritional factors tailored to different food matrices and diverse gastrointestinal environments, enhancing their bioavailability and maintaining human health.

CRediT authorship contribution statement

Wenjun Li: Writing – original draft, Resources, Project administration, Methodology, Conceptualization. **Qianqian Bie:** Methodology, Investigation, Formal analysis, Data curation. **Kaihui Zhang:** Methodology, Investigation, Formal analysis, Data curation. **Fangzhou Linli:** Methodology, Investigation, Data curation. **Wenyu Yang:** Writing – review & editing, Supervision, Resources, Funding acquisition. **Xianggui Chen:** Supervision, Funding acquisition. **Pengfei Chen:** Supervision, Funding acquisition. **Qi Qi:** Methodology, Investigation.

Declaration of competing interest

The authors declare that they have no known competing financial interests or personal relationships that could have appeared to influence the work reported in this paper. The authors appreciate the support provided by the Science and Technology Program of Sichuan Province (2023NSFSC1206, 2022YFN0016), and the Frontiers Medical Center, Tianfu Jincheng Laboratory Foundation (TFJC2023010008), Sichuan Provincial Administration of Traditional Chinese Medicine (2021MS232), the Key Laboratory of National Forestry and Grassland Administration on Highly-Efficient Utilization of Forestry Biomass Resources in Southwest China (2023-KF02), Southwest Forestry University, and Xihua University Science and Technology Innovation Competition Project for Postgraduate Students (YK20240258).

Data availability

Data will be made available on request.

References

Ahmad, M., Ashraf, B., Gani, A., & Gani, A. (2018). Microencapsulation of saffron anthocyanins using β glucan and β cyclodextrin: Microcapsule characterization, release behaviour & antioxidant potential during in-vitro digestion. *International Journal of Biological Macromolecules, 109*, 435–442. https://doi.org/10.1016/j.ijbiomac.2017.11.122

Altunbas, A., Lee, S. J., Rajasekaran, S. A., Schneider, J. P., & Pochan, D. J. (2011). Encapsulation of curcumin in self-assembling peptide hydrogels as injectable drug delivery vehicles. *Biomaterials, 32*(25), 5906–5914. https://doi.org/10.1016/j.biomaterials.2011.04.069

Bardajee, G. R., Khamooshi, N., Nasri, S., & Vancaeyzeele, C. (2020). Multi-stimuli responsive nanogel/hydrogel nanocomposites based on kappa-carrageenan for prolonged release of levodopa as model drug. *International Journal of Biological Macromolecules, 153*, 180–189. https://doi.org/10.1016/j.ijbiomac.2020.02.329

Bobinaitė, R., Viškelis, P., & Venskutonis, P. R. (2012). Variation of total phenolics, anthocyanins, ellagic acid and radical scavenging capacity in various raspberry (Rubus spp.) cultivars. *Food Chemistry, 132*(3), 1495–1501. https://doi.org/10.1016/j.foodchem.2011.11.137

Cai, D., Li, X., Chen, J., Jiang, X., Ma, X., Sun, J., et al. (2022). A comprehensive review on innovative and advanced stabilization approaches of anthocyanin by modifying structure and controlling environmental factors. *Food Chemistry, 366*, 130611–130623. https://doi.org/10.1016/j.foodchem.2021.130611

Cui, H., Jiang, Q., Gao, N., Tian, J., Wu, Y., Li, J., et al. (2024). Complexes of glycated casein and carboxymethyl cellulose enhance stability and control release of anthocyanins. *Food Research International, 176*, Article 113804. https://doi.org/10.1016/j.foodres.2023.113804

Dong, H., Wang, M., Fan, S., Wu, C., Zhang, C., Wu, X., et al. (2022). Redox-regulated conformational change of disulfide-rich assembling peptides. *Angewandte Chemie, International Edition, 61*(44), Article e202212829. https://doi.org/10.1002/anie.202212829

Gui, H., Sun, L., Liu, R., Si, X., Li, D., Wang, Y., et al. (2023). Current knowledge of anthocyanin metabolism in the digestive tract: Absorption, distribution, degradation, and interconversion. *Critical Reviews in Food Science and Nutrition, 63*(22), 5953–5966. https://doi.org/10.1080/10408398.2022.2026291

He, B., Ge, J., Yue, P., Yue, X., Fu, R., Liang, J., et al. (2017). Loading of anthocyanins on chitosan nanoparticles influences anthocyanin degradation in gastrointestinal fluids and stability in a beverage. *Food Chemistry, 221*, 1671–1677. https://doi.org/10.1016/j.foodchem.2016.10.120

Hu, Y., & Ying, J. Y. (2023). Reconfigurable A-motif, i-motif and triplex nucleic acids for smart pH-responsive DNA hydrogels. *Materials Today, 63*, 188–209. https://doi.org/10.1016/j.mattod.2022.12.003

Jeong, D., & Na, K. (2012). Chondroitin sulfate based nanocomplex for enhancing the stability and activity of anthocyanin. *Carbohydrate Polymers, 90*(1), 507–515. https://doi.org/10.1016/j.carbpol.2012.05.072

Jiang, Q., Zhang, M., Mujumdar, A. S., & Chen, B. (2023). Effects of electric and magnetic field on freezing characteristics of gel model food. *Food Research International, 166*, Article 112566. https://doi.org/10.1016/j.foodres.2023.112566

Jin, W., Xiang, L., Peng, D., Liu, G., He, J., Cheng, S., et al. (2020). Study on the coupling progress of thermo-induced anthocyanins degradation and polysaccharides gelation. *Food Hydrocolloids, 105*, 105822–105827. https://doi.org/10.1016/j.foodhyd.2020.105822

Kim, Y., Hwang, S., Khalmuratova, R., Kang, S., Lee, M., Song, Y., et al. (2020). α-Helical cell-penetrating peptide-mediated nasal delivery of resveratrol for inhibition of epithelial-to-mesenchymal transition. *Journal of Controlled Release, 317*, 181–194. https://doi.org/10.1016/j.jconrel.2019.11.034

Lang, Y., Li, B., Gong, E., Shu, C., Si, X., Gao, N., et al. (2021). Effects of alpha-casein and beta-casein on the stability, antioxidant activity and bioaccessibility of blueberry anthocyanins with an in vitro simulated digestion. *Food Chemistry, 334*, 127526–127533. https://doi.org/10.1016/j.foodchem.2020.127526

Li, W., Linli, F., Yang, W., & Chen, X. (2023). Enhancing the stability of natural anthocyanins against environmental stressors through encapsulation with synthetic peptide-based gels. *International Journal of Biological Macromolecules, 253*, 127133–127143. https://doi.org/10.1016/j.ijbiomac.2023.127133

Li, W., Wang, D., Shi, X., Li, J., Ma, Y., Wang, Y., et al. (2018). A siRNA-induced peptide co-assembly system as a peptide-based siRNA nanocarrier for cancer therapy. *Materials Horizons, 5*(4), 745–752. https://doi.org/10.1039/C9MH90031D

Liu, L., Zhang, D., Song, X., Guo, M., Wang, Z., Geng, F., et al. (2022). Compound hydrogels derived from gelatin and gellan gum regulates the release of anthocyanins in simulated digestion. *Food Hydrocolloids, 127*, 107487–107496. https://doi.org/10.1016/j.foodhyd.2022.107487

Luo, S. Z., Hu, X. F., Pan, L. H., Zheng, Z., Zhao, Y. Y., Cao, L. L., et al. (2019). Preparation of camellia oil-based W/O emulsions stabilized by tea polyphenol palmitate: Structuring camellia oil as a potential solid fat replacer. *Food Chemistry, x276*, 209–217. https://doi.org/10.1016/j.foodchem.2018.09.161

Mandru, M., Bercea, M., Gradinaru, L. M., Ciobanu, C., Drobota, M., Vlad, S., et al. (2019). Polyurethane/poly(vinyl alcohol) hydrogels: Preparation, characterization and drug delivery. *European Polymer Journal, 118*, 137–145. https://doi.org/10.1016/j.eurpolymj.2019.05.049

Ozel, B., Aydin, O., & Oztop, M. H. (2020). In vitro digestion of polysaccharide including whey protein isolate hydrogels. *Carbohydrate Polymers, 229*, 115469–115482. https://doi.org/10.1016/j.carbpol.2019.115469

Peng, Z., Peng, Z., & Shen, Y. (2011). Study on biological safety of polyvinyl alcohol/collagen hydrogel as a tissue substitute (II). *Journal of Macromolecular Science, Part A, 48*(8), 632–636.

Song, J., Zhang, C., Kong, S., Liu, F., Hu, W., Su, F., et al. (2022). Novel chitosan based metal-organic polyhedrons/enzyme hybrid hydrogel with antibacterial activity to promote wound healing. *Carbohydrate Polymers, 291*, Article 119522. https://doi.org/10.1016/j.carbpol.2022.119522

Tai, M. R., Ji, H. W., Chen, J. P., Liu, X. F., Song, B. B., Zhong, S. Y., et al. (2023). Biomimetic triumvirate nanogel complexes via peptide-polysaccharide-polyphenol self-assembly. *International Journal of Biological Macromolecules, 251*, 126232–126241. https://doi.org/10.1016/j.ijbiomac.2023.126232

Tena-Solsona, M., Alonso-de Castro, S., Miravet, J. F., & Escuder, B. (2014). Co-assembly of tetrapeptides into complex pH-responsive molecular hydrogel networks. *Journal of Materials Chemistry B, 2*(37), 6192–6197. https://doi.org/10.1039/C4TB00795F

Victoria-Campos, C. I., Ornelas-Paz, J.d. J., Rocha-Guzmán, N. E., Gallegos-Infante, J. A., Failla, M. L., Pérez-Martínez, J. D., et al. (2022). Gastrointestinal metabolism and bioaccessibility of selected anthocyanins isolated from commonly consumed fruits. *Food Chemistry, 383*, Article 132451. https://doi.org/10.1016/j.foodchem.2022.132451

Wang, L., Dong, Y., Wang, L., Cui, M., Zhang, Y., Jiang, L., et al. (2023). Elucidating the effect of the Hofmeister effect on formation and rheological properties of soy protein/κ-carrageenan hydrogels. *Food Hydrocolloids, 143*, Article 108905. https://doi.org/10.1016/j.foodhyd.2023.108905

Wang, Y., Li, Z., Bao, Y., Cui, H., Li, J., Song, B., et al. (2023). Colon-targeted delivery of polyphenols: Construction principles, targeting mechanisms and evaluation methods. *Critical Reviews in Food Science and Nutrition*, 1–23. https://doi.org/10.1080/10408398.2023.2266842

Wei, D., Liu, Q., Liu, Z., Liu, J., Zheng, X., Pei, Y., et al. (2019). Modified nano microfibrillated cellulose/carboxymethyl chitosan composite hydrogel with giant network structure and quick gelation formability. *International Journal of Biological Macromolecules, 135*, 561–566. https://doi.org/10.1016/j.ijbiomac.2019.05.091

Yang, Y., Feng, G., Wang, J., Zhang, R., Zhong, S., Wang, J., et al. (2023). Injectable chitosan-based self-healing supramolecular hydrogels with temperature and pH dual-responsivenesses. *International Journal of Biological Macromolecules, 227*, 1038–1047. https://doi.org/10.1016/j.ijbiomac.2022.11.279

Yao, L., Xu, J., Zhang, L., Liu, L., & Zhang, L. (2021). Nanoencapsulation of anthocyanin by an amphiphilic peptide for stability enhancement. *Food Hydrocolloids, 118*, Article 106741. https://doi.org/10.1016/j.foodhyd.2021.106741

Zhang, B., Li, X., Xie, Q., Tao, H., Wang, W., & Chen, H.-Q. (2017). Preparation and characterization of non-crystalline granular starch and corresponding carboxymethyl starch. *International Journal of Biological Macromolecules, 103*, 656–662. https://doi.org/10.1016/j.ijbiomac.2017.05.131

Zhang, L., Yao, L., Zhao, F., Yu, A., Zhou, Y., Wen, Q., et al. (2023). Protein and peptide-based nanotechnology for enhancing stability, bioactivity, and delivery of anthocyanins. *Advanced Healthcare Materials, 12*(25). https://doi.org/10.1002/adhm.202300473

Zhao, L., Pan, F., Mehmood, A., Zhang, H., Rehman, A. U., Li, J., et al. (2021). Improved color stability of anthocyanins in the presence of ascorbic acid with the combination of rosmarinic acid and xanthan gum. *Food Chemistry, 351*, Article 129317. https://doi.org/10.1016/j.foodchem.2021.129317

Zhao, X., Zhang, X., Tie, S., Hou, S., Wang, H., Song, Y., et al. (2020). Facile synthesis of nano-nanocarriers from chitosan and pectin with improved stability and biocompatibility for anthocyanins delivery: An in vitro and in vivo study. *Food Hydrocolloids, 109*, 106114–106124. https://doi.org/10.1016/j.foodhyd.2020.106114